

Small functional groups for controlled differentiation of hydrogel-encapsulated human mesenchymal stem cells

DANIELLE S. W. BENOIT¹, MICHAEL P. SCHWARTZ^{1,2}, ANDREW R. DURNEY¹ AND KRISTI S. ANSETH^{1,2*}

¹Department of Chemical and Biological Engineering, University of Colorado, 424 UCB ECCH 111, Boulder, Colorado 80309, USA

²Howard Hughes Medical Institute, University of Colorado, 424 UCB ECCH 111, Boulder, Colorado 80309, USA

*e-mail: Kristi.anseth@colorado.edu

Published online: 24 August 2008; doi:10.1038/nmat2269

Cell–matrix interactions have critical roles in regeneration, development and disease. The work presented here demonstrates that encapsulated human mesenchymal stem cells (hMSCs) can be induced to differentiate down osteogenic and adipogenic pathways by controlling their three-dimensional environment using tethered small-molecule chemical functional groups. Hydrogels were formed using sufficiently low concentrations of tether molecules to maintain constant physical characteristics, encapsulation of hMSCs in three dimensions prevented changes in cell morphology, and hMSCs were shown to differentiate in normal growth media, indicating that the small-molecule functional groups induced differentiation. To our knowledge, this is the first example where synthetic matrices are shown to control induction of multiple hMSC lineages purely through interactions with small-molecule chemical functional groups tethered to the hydrogel material. Strategies using simple chemistry to control complex biological processes would be particularly powerful as they could make production of therapeutic materials simpler, cheaper and more easily controlled.

Interactions of cells and extracellular matrix (ECM) initiate signalling cascades involved in critical cell functions, such as regeneration^{1–3}. An important goal of tissue engineering is to mimic critical aspects of the extracellular environment and to control cell function through cell–material interactions⁴. The complexity of natural ECM and cell–matrix interactions makes design of materials for regenerative medicine applications challenging because a variety of factors will influence cell fate. The choice of the chemical environment used for a specific tissue engineering application is dependent on the desired outcome, and many studies have shown that chemical functionality and hydrophilicity have important roles in cell adhesion and function^{5–10}. Comprehensive studies have also demonstrated that surface function of two-dimensional (2D) materials has a role in differentiation of embryonic stem cells down the hepatocyte lineage based on ECM protein presentation¹¹ and epithelial lineage based on charge, hydrophilicity and branching⁵. The attachment and growth of human mesenchymal stem cells (hMSCs), the control of neural stem cell differentiation, and articular chondrocyte function, have also been studied¹². However, conclusions about the specific effects of chemical functionalities using approaches so far are complicated^{5,12}, especially on 2D surfaces, because factors such as stiffness and or cell spreading can be influenced by the charge and hydrophilicity of the surface, and these factors have been shown to have a significant influence on stem cell fate^{13,14}.

The goal of this work was to identify tethered chemical functional groups that could influence differentiation of hMSCs owing to the importance of this cell type in potential regenerative medicine applications^{15–17}. Our strategy was to screen immobilized small molecules for their ability to induce hMSCs to differentiate down pathways important for tissue engineering. The small molecules were chosen to incorporate functionalities found in the

extracellular environment of the hMSC target cell types. Initial screening for differentiation markers was carried out on 2D arrays, and the results were used to design 3D encapsulation materials for inducing hMSC differentiation. We were able to formulate 3D encapsulation materials that had functional groups with different charge and hydrophilicity, but at concentrations of tether molecules that did not affect materials properties such as stiffness and swelling. Furthermore, by encapsulating hMSCs in these materials, they were trapped in a rounded morphology that was the same for each of the materials tested. Finally, encapsulated hMSCs were cultured in standard hMSC media, without added cytokines or steroids typically used in differentiation media. As a result, we were able to definitively demonstrate that tethered small molecules could indeed have a direct influence on the differentiation fate of hMSCs, with charged phosphate groups leading to osteogenesis and hydrophobic *t*-butyl groups inducing adipogenesis. This work demonstrates that biomaterials with very simple functionalities may be used to control complicated cellular function such as stem cell differentiation, a result that could have interesting fundamental implications, but more importantly could lead to simple, cheap, highly controllable biomaterials formulations for controlling differentiation of hMSCs for regenerative medicine applications.

As an initial screening tool to identify promising hydrogel formulations, hMSCs were cultured on arrays of poly(ethylene glycol) (PEG) functionalized with various small molecules (Fig. 1a). Taking advantage of the 2D experimental design, immunostaining was used to determine concentrations of small-molecule functionalization that induced elevated expression of proteins important for chondrogenesis, osteogenesis and adipogenesis. Promising immunostaining formulations were then further screened using fluorescent *in situ* hybridization (FISH) analysis to ultimately identify formulations for 3D encapsulation

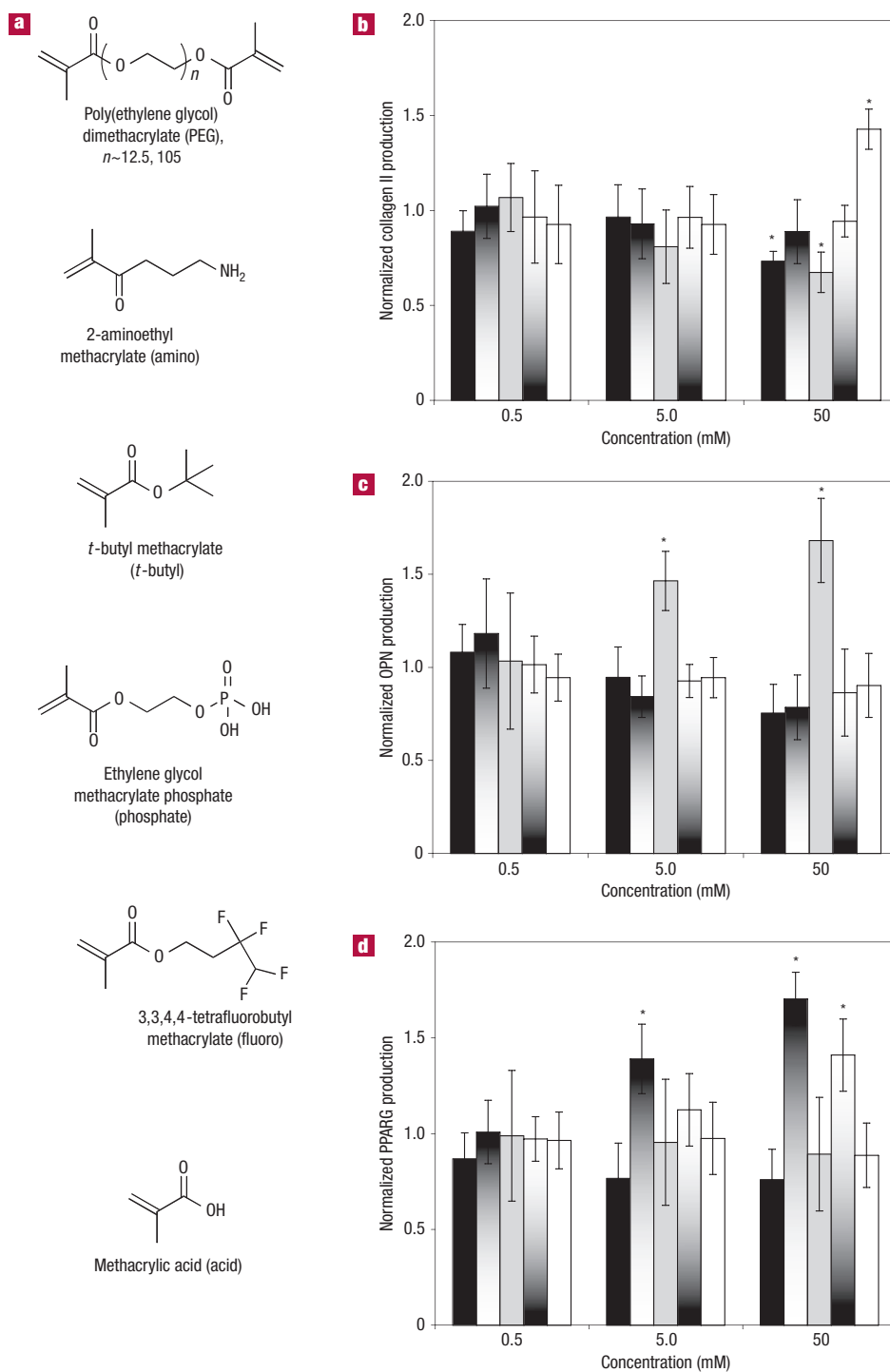


Figure 1 Small-molecule incorporation alters hMSC protein expression on PEG hydrogels. **a–d**, Chemical structures of functional moieties incorporated (**a**) and protein expression of hMSCs (as measured by immunostaining) quantitatively analysed for collagen II (**b**), OPN (**c**) and PPARG (**d**) after 10 days of culture in control media on unmodified PEG and 0.5, 5 and 50 mM of amino (black bars), *t*-butyl (black (top) to white (bottom) gradient bars), phosphate (grey bars), fluoro (white (top) to black (bottom) gradient bars) and acid (white bars). Values are reported as the fluorescent intensity average of six samples per composition, relative to the number of cells, as analysed by propidium iodide counterstaining, and normalized to expression by cells cultured on PEG surfaces. Error bars represent one standard deviation. An asterisk (*) denotes statistical significance compared with PEG ($p < 0.05$).

experiments. As the goal of this work was to identify 3D encapsulation materials, a complete evaluation of differentiation on 2D surfaces was not carried out. Small molecules were chosen

to capture chemical aspects of the native extracellular space of relevant tissues to determine if differentiation could be controlled through cell–material interactions. Carboxylic acid functionalities

resemble the exposed functional groups of native cartilage, which is rich in glycosaminoglycans¹⁸, phosphates were chosen because they have an important role in mineralized tissue development such as bone formation^{10,19} and hydrophobic functional groups were chosen because adipose cells are rich in lipids²⁰ and release fatty acids into their extracellular space²¹.

Figure 1b–d summarizes the immunostaining results for hMSCs cultured on various concentrations of the different functional moieties (the array design used is shown in Supplementary Information, Fig. S1). Cultured hMSCs were monitored at day 10 using immunostaining of collagen II, osteopontin (OPN) and peroxisome proliferating antigen receptor gamma (PPARG). Collagen II is the major extracellular component of cartilage and an indicator of chondrogenesis, OPN is an ECM protein found in bone and was monitored as a measure of osteogenesis and PPARG is a critical regulator of adipogenesis.

A detailed explanation of 2D immunostaining results can be found in the Supplementary Information. Briefly, Fig. 1b demonstrates that, whereas there is no change for collagen II production at the lower concentrations, an increase was observed for 50 mM acid-functionalized surfaces relative to the control gel (0 mM). Whereas OPN was unchanged for most treatments, hMSCs cultured on phosphate-functionalized gels showed increased OPN production at 5 and 50 mM concentrations relative to the control gel. The hydrophobic *t*-butyl- and fluoro-functionalized hydrogels elicited elevated expression of PPARG by hMSCs at 5 mM and the greatest expression at the 50 mM concentration relative to the control gel, whereas the other gels remained unchanged or decreased expression. In summary, for each of the surfaces, the 50 mM concentration led to the biggest increase in expression of markers for differentiation; acid-functionalized gels increased the chondrogenic marker collagen II, phosphate-functionalized gels increased the osteogenic marker OPN and hydrophobic surfaces, especially the *t*-butyl surface, increased the adipogenic marker PPARG.

Figure 2 summarizes the results for FISH analysis of hMSC differentiation based on hydrogel formulations with the highest functional group concentration, 50 mM as this concentration showed the highest increases in expression by immunostaining. For FISH analysis, we monitored expression of aggrecan, a component of cartilage ECM and an early indicator of chondrogenic differentiation (Fig. 2a), CBFA1 gene expression as a measurement of osteogenic differentiation (Fig. 2b) and PPARG as a measure of adipogenic differentiation (Fig. 2c). A detailed summary of the FISH results can be found in the Supplementary Information. Briefly, aggrecan was unchanged for all treatments at day 0, but was found to be produced at constant or decreased levels relative to control gels for cells cultured on all surfaces at day 4 (Fig. 2a). By day 10, all surfaces exhibited decreased aggrecan expression, except for the acid-functionalized gel, which exhibited elevated expression. At day 0, hMSCs showed no significant CBFA1 expression differences; however, at day 4, cells cultured on phosphate-functionalized hydrogel spots exhibited a twofold increase of CBFA1 gene expression over poly(ethylene glycol) dimethacrylate (PEG) alone, whereas the other surfaces led to the same or decreased expression. At day 10, the CBFA1 gene expression of hMSCs seeded on phosphate-functionalized gels showed a large increase compared with PEG; fluoro-functionalized gels also demonstrated a moderate increase in CBFA1 gene expression whereas the other gels demonstrated decreased expression. Only hydrophobic *t*-butyl and fluoro groups exhibited increased PPARG expression at day 4 and day 10. Taken together, protein production and gene expression demonstrate that hMSCs cultured in the presence of 50 mM acid, phosphate and *t*-butyl groups promote the expression of markers that can be associated

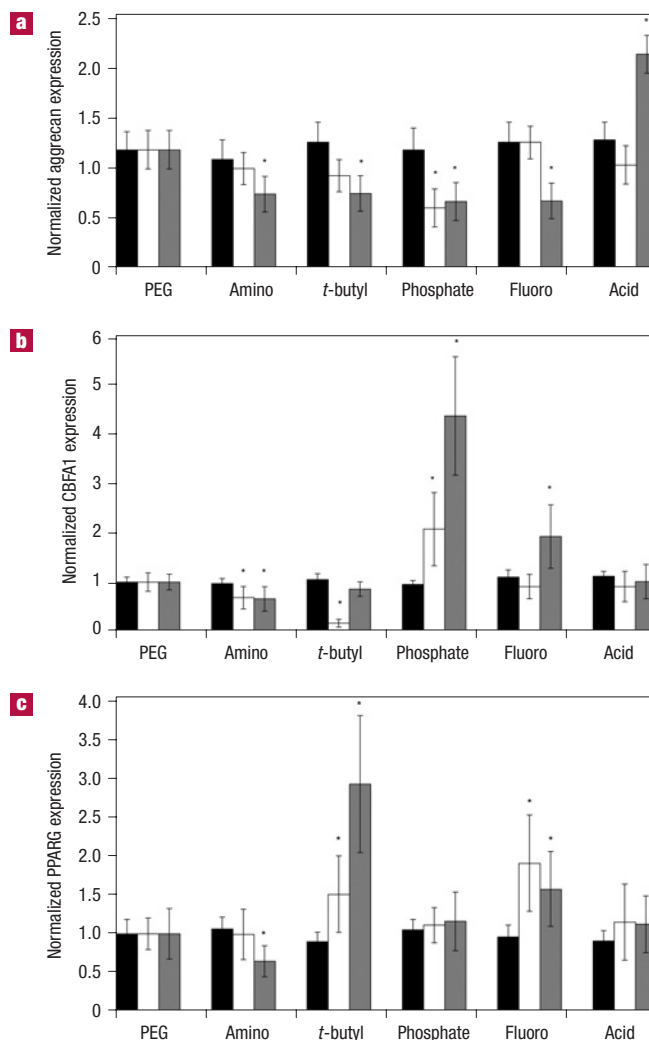


Figure 2 Small-molecule incorporation alters hMSC gene expression on PEG hydrogels. **a–c**, Gene expression of hMSCs (as measured by *in situ* hybridization) quantitatively analysed for aggrecan (**a**), CBFA1 (**b**) and PPARG (**c**) at days 0 (black bars), 4 (white bars) and 10 (grey) of culture on unmodified PEG and 50 mM of amino, *t*-butyl, phosphate, fluoro and acid. Values are reported as the fluorescent intensity average of six samples per composition per time point, relative to β -actin expression, and normalized to expression by cells cultured on PEG surfaces. Error bars represent one standard deviation. An asterisk (*) denotes statistical significance compared with PEG ($p < 0.05$).

with differentiation pathways of chondrocytes, osteoblasts and adipocytes, respectively.

Morphological characteristics of hMSCs cultured on acid-, phosphate- and *t*-butyl-functionalized surfaces suggest chondrogenic, osteogenic and adipogenic phenotypes as well. Figure 3 shows light micrographs (Fig. 3a–d) and F-actin immunostaining (Fig. 3e–h) for hMSCs cultured on PEG (Fig. 3a,e) and 50 mM acid- (Fig. 3b,f), phosphate- (Fig. 3c,g) and *t*-butyl- (Fig. 3d,h) functionalized surfaces. The image in Fig. 3b and the F-actin staining shown in Fig. 3f demonstrate that hMSCs exhibit a round morphology on the acid-terminated surface, reminiscent of two-dimensionally cultured chondrocytes^{22,23}. hMSCs cultured on phosphate hydrogel surfaces exhibit a similarly spread morphology to *in vitro* osteoblasts (light

micrograph, Fig. 3c and F-actin staining, Fig. 3g), which is consistent with the hypothesis that phosphate-functionalization may promote osteogenesis. In addition to increased adipogenic protein expression, cells seeded on gels containing hydrophobic functional groups also seem morphologically similar to adipocytes, including evidence of the formation of intracellular lipid droplets (grey deposits shown in Fig. 3d). Moreover, hMSCs cultured on *t*-butyl-functionalized gels are significantly less spread (light micrograph, Fig. 3d and F-actin staining, Fig. 3h) than hMSCs cultured on PEG and have very few projections, similar to adipocytes. Therefore, on the basis of immunostaining, FISH and morphological characteristics, we were able to identify promising formulations for testing small-molecule-functionalized hydrogels for induced differentiation of encapsulated hMSCs.

Ultimately, we aim to discover materials that promote hMSC differentiation down specific, tissue-related pathways. We tested the most promising formulations identified using the 2D arrays to determine if a 3D hydrogel environment could be accurately predicted to promote specific hMSC differentiation. Specifically, we chose to encapsulate hMSCs in *t*-butyl- and phosphate-functionalized hydrogels to test for osteogenic and adipogenic differentiation, respectively, without the use of differentiation media. The 3D environment enables hMSCs to be encapsulated at a fixed density for all gel compositions, and all of the cells are maintained in a similar rounded morphology, enabling the effects of the chemical functionality on hMSC differentiation to be tested in the absence of these variations that often occur on 2D surfaces. Immunoblotting was used to evaluate osteogenic and adipogenic markers, and histology and immunohistochemistry were carried out on the constructs after 21 days of encapsulation to examine the distribution and components of elaborated matrix.

Immunoblotting of CBFA1 and PPARG was carried out to evaluate osteogenesis and adipogenesis, respectively. Figure 4 shows the results (Fig. 4a) and quantification (Fig. 4b,c) for hMSCs encapsulated in *t*-butyl-, phosphate-functionalized and control PEG hydrogels after 0, 4, 10 and 21 days of culture. Immunoblots (Fig. 4b) for hMSCs encapsulated in phosphate-functionalized hydrogels identify detectable upregulation of CBFA1 after 10 days in culture, with further increases observed at day 21, indicating differentiation down an osteogenic pathway. For *t*-butyl-functionalized hydrogels, PPARG production was upregulated starting at day 10 and remained constant to day 21, suggesting increased hMSC adipogenesis (Fig. 4c).

Standard histological staining as well as immunohistochemistry indicative of osteogenesis or adipogenesis was used to evaluate specific matrix production by encapsulated hMSCs. Masson's trichrome, which stains collagen blue, muscle and cytoplasm red and nuclei black, was used to verify osteogenic differentiation. Figure 4d illustrates that Masson's trichrome staining (left column) shows very little collagen or muscle tissue development by cells encapsulated in PEG or in *t*-butyl-functionalized hydrogels. In contrast, hMSCs cultured in phosphate-functionalized hydrogels produce a collagen-rich matrix, deposited pericellularly, which is common for non-degradable hydrogels such as those used here^{24,25}. Immunohistochemical staining of the bone matrix extracellular protein, osteopontin, revealed very little to no staining for PEG or *t*-butyl-functionalized gels. However, hMSCs cultured in phosphate-functionalized hydrogels elaborated a fairly rich matrix of osteopontin, as shown by the nearly uniform light brown staining (Fig. 4d, second column). Bone tissue is composed of a rich collagen matrix and other structural proteins such as osteopontin with hydroxylapatite mineral deposits. The development of a collagen- and osteopontin-rich matrix by hMSCs encapsulated in phosphate-functionalized hydrogels supports the assignment of osteogenic differentiation as determined through immunoblotting.

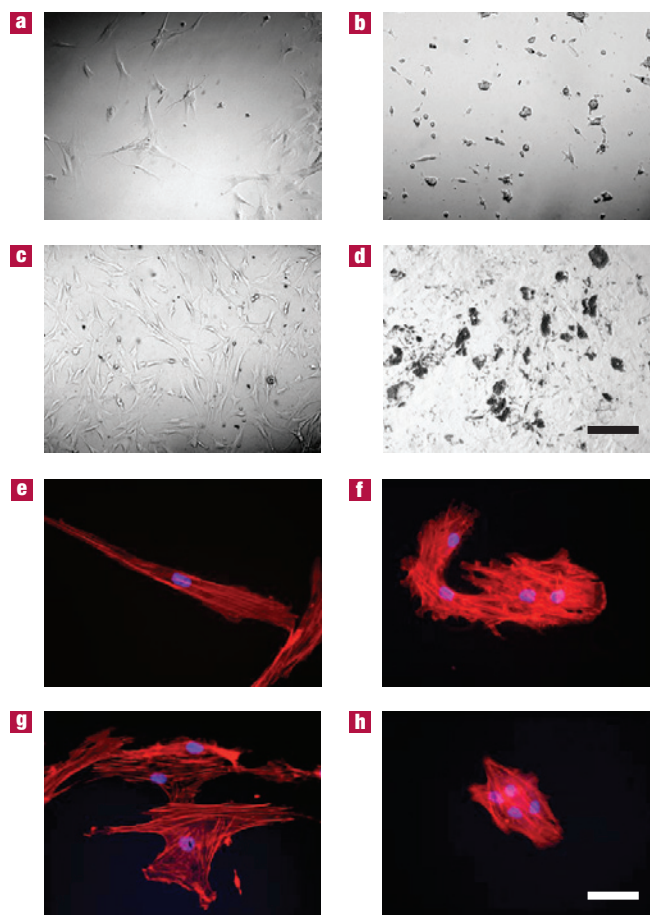


Figure 3 hMSC morphology is altered in response to small-molecule incorporation into PEG hydrogels. **a–h**, Representative light and fluorescent micrographs of TRITC-phalloidin- (red) and DAPI- (blue) stained hMSCs showing morphology cultured on PEG (**a** and **e**), acid- (**b** and **f**), phosphate- (**c** and **g**) and *t*-butyl- (**d** and **h**) functionalized surfaces (scale bar = 200 μm for light micrographs, scale bar = 50 μm for fluorescent micrographs).

Oil red, which stains intracellular lipid deposits red, was used to verify adipogenesis. Oil-red staining is negative for PEG and phosphate-functionalized hydrogels but positive for hMSCs cultured within *t*-butyl-functionalized hydrogels (Fig. 4d, third column). As adipogenesis proceeds, cells accumulate lipids intracellularly, and therefore the presence of Oil-red-positive staining for hMSCs cultured in *t*-butyl-functionalized PEG hydrogels is indicative of adipogenic differentiation. Furthermore, the distribution of PPARG was examined. Whereas PEG and phosphate-functionalized hydrogels showed no PPARG staining, *t*-butyl-functionalized hydrogels showed robust PPARG staining (Fig. 4d, right column), and, as PPARG is a regulator of adipogenic differentiation, this serves as strong evidence that the *t*-butyl functionalities are promoting adipogenesis. Therefore, we conclude that, on the basis of immunoblotting, histology and immunohistochemistry results, 3D encapsulation of hMSCs in phosphate- and *t*-butyl-functionalized PEG hydrogels leads to osteogenic and adipogenic differentiation, respectively.

Signals from the ECM, such as physical structure and chemical environment, are known to have a critical role in guiding stem cell differentiation^{26,27}, but the complexity of the native ECM is difficult

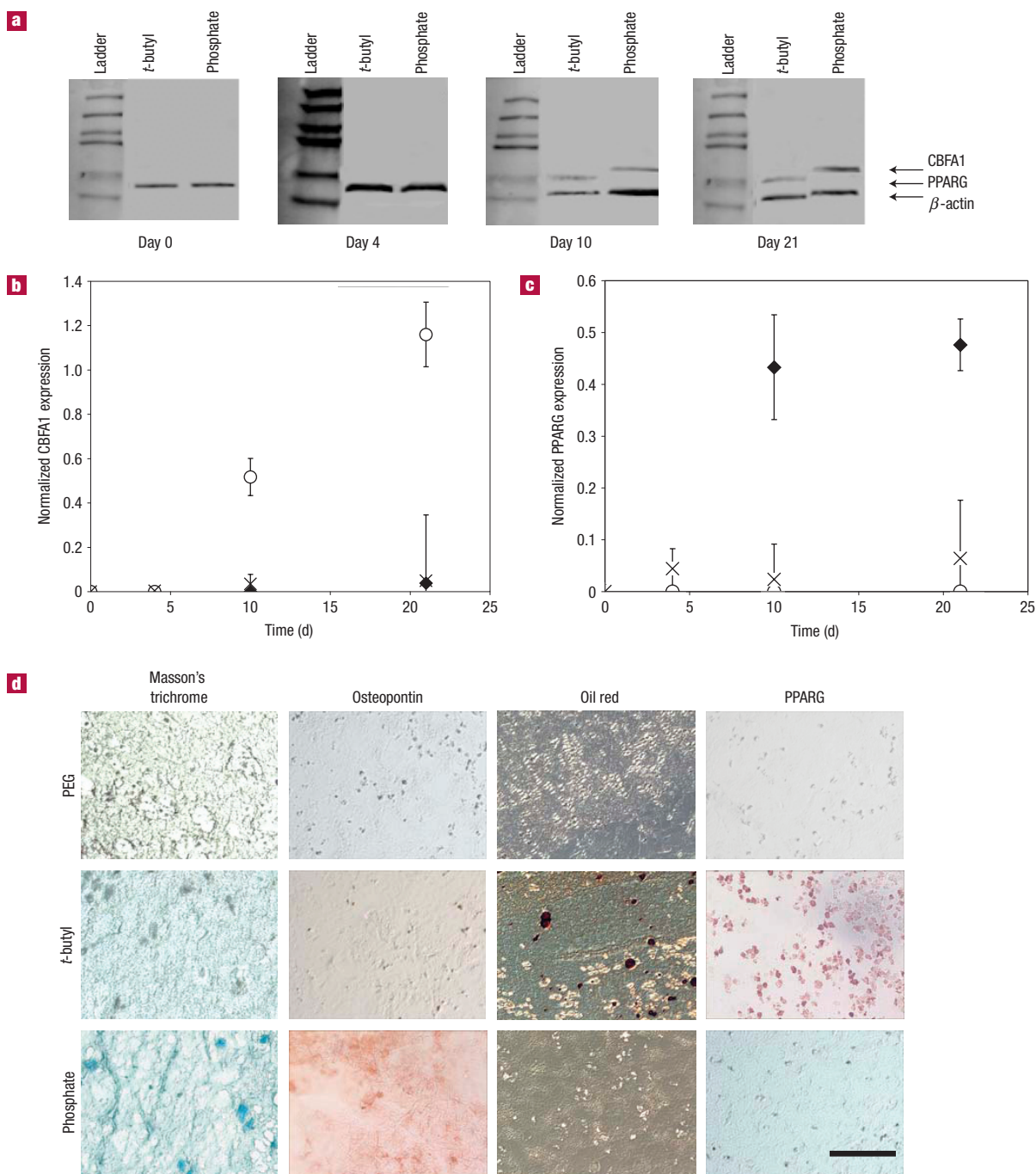


Figure 4 Encapsulation of hMSCs in phosphate- and *t*-butyl-functionalized PEG hydrogels induces MSC osteogenesis and adipogenesis, respectively. CBFA1, PPARG and β -actin expression of hMSCs encapsulated in control, *t*-butyl- and phosphate-functionalized PEG hydrogels and cultured for 0, 4, 10 and 21 days in control media. **a–c**, Immunoblots (**a**) were quantified with ImageJ software and CBFA1 (**b**) and PPARG (**c**) expression levels over the 21-day culture period were normalized to β -actin expression (PEG: crosses; *t*-butyl-functionalized: filled diamonds; phosphate-functionalized: open circles), error bars represent one standard deviation. **d**, Differentiation was further verified using histological and immunohistochemistry staining of matrix evolution by encapsulated hMSCs. Masson's trichrome stains collagen blue (left column) and Oil red stains intracellular lipid deposits red (third column). OPN and PPARG staining was carried out using protein-specific primary antibodies and horseradish-peroxidase-labelled secondaries, and visualized with Vector NovaRed Substrate Kit (Vector Labs) (scale bar = 100 μ m).

or impossible to completely recreate synthetically. Therefore, there is a great deal of motivation to identify simplified synthetic mimetics for guiding differentiation down specific phenotypic pathways. Screening materials based on knowledge about the tissue

environment in which a stem cell resides and choosing chemical strategies accordingly could therefore have a significant impact on tissue engineering strategies. Phosphates, typically calcium phosphate, are widely used osteoconductive and osteoinductive

materials in which sequestering of charged proteins, such as the acidic sialoprotein osteopontin, leads to subsequent adhesion and promotion of osteogenesis of hMSCs. Phosphates have an important role in mineralized tissue development^{10,19}, and when incorporated into biomaterial scaffolds, may promote differentiation, as well as nucleation and mineral deposit formation¹⁰. Cell attachment is characterized by binding of integrin receptors to molecules of the ECM, and the dynamic interaction of focal adhesions with the underlying substrate is significant for integrin-mediated signal transduction and the biological response of the cell.

During adipogenesis, ECM remodelling defines the onset of the differentiation process. Remodelling during adipogenesis is characterized by the conversion of a fibronectin-rich stromal matrix of the pre-adipocyte to the basement membrane of an adipocyte^{28–30}. The expression of ECM components is highly regulated during the process of adipocyte differentiation: types I and III collagen, fibronectin and β 1-integrins are downregulated, whereas type-IV collagen and entactin are upregulated³¹. Also important for MSC adipogenesis is ECM-regulated cell morphology. Growth of pre-adipocytes on a matrix that induces a spread cell morphology inhibits adipocyte differentiation, and this effect is overcome by the disruption of actin filaments, which promotes rounding-up of cells³². Thus, both ECM production and cell morphology have roles in MSC adipogenesis.

For the 3D studies presented here, cells are entrapped in a rounded morphology, which would be expected to be beneficial for adipogenesis. Our results indicate that phosphate-functionalized PEG hydrogels induce osteogenesis, whereas *t*-butyl-functionalized hydrogels induce adipogenesis. Deconvoluting the role of cell morphology from cell–matrix interactions is difficult in 2D studies, but a 3D PEG environment restricts spreading of encapsulated cells, owing to the small mesh size. Thus, the role of the cell–matrix interactions can be more directly studied. As adipogenesis is more efficient when cells adopt a rounded morphology³², encapsulation in a hydrogel may actually further enhance differentiation. Spreading may be less crucial for osteogenesis, as hMSC osteogenic differentiation is observed for rounded cells in 3D. Although matrix formation is also likely to have a role in hMSC fate for cells encapsulated in functionalized PEG gels, these cells only see a simplified chemical environment at early time points. Therefore, on the basis of the fact that phosphate groups promote osteogenesis whereas *t*-butyl groups promote adipogenesis, it is possible that initial interactions between functionalized PEG gels and hMSCs are sufficient for determining the ultimate fate of the stem cell.

Chemically, *t*-butyl groups and phosphate groups have very different properties, although at the concentrations used, the overall physical properties of the PEG gels were unchanged. Our results indicate that hMSCs differentiate down adipogenic or osteogenic pathways for *t*-butyl or phosphate functionalization, leading to cell-specific matrix production (Fig. 4). One possible explanation for our observations may be that tethered chemical groups lead to direct cell–matrix interactions that induce differentiation down pathways that lead to production of tissue-specific matrix molecules. Alternatively, specific chemical interactions may nucleate the sequestering of only particular cell-secreted molecules, and the subsequent matrix formation may then direct differentiation. In either case, the matrix produced by the hMSCs would then interact with the cells in a more complex way that supports differentiation down a specific pathway. These results could have profound implications for tissue engineering strategies using synthetic materials, because they suggest that it may only be necessary to control initial elements of cell expression to guide more complex overall processes.

Understanding the role of the ECM environment and recreating the important aspects of the natural cellular niche are critical for

materials-based, tissue engineering approaches to be successful. The approach reported here provides a method for initially screening chemical or biological factors important to recreating the ECM environment, because the PEG-based chemistry enables the incorporation of a broad range of biologically relevant molecules such as proteins, peptides and glycosaminoglycans^{24,33–41}. So far, much of the high-throughput research carried out on stem cells has focused on soluble signals and their subsequent effects on cellular functions²⁷. Our approach presents a method for studying the context in which the cells are screened by controlling the local microenvironment, thereby enabling an improved understanding of the effects of extracellular interactions on cell activities in the presence and absence of soluble signals.

Collectively, we demonstrate that rational design can be used to identify synthetic extracellular environments that induce differentiation of hMSCs down specific target pathways using small-molecule chemical moieties even when mechanistic details are unknown. Of particular importance is the fact that cell–material interactions can be identified as having a crucial role in cell fate because the differentiation pathways were induced using normal hMSC growth media, in the absence of soluble signals. Previously, differentiation of embryonic stem cells was induced by biological and physical cues⁵, and material compliance was shown to induce hMSC differentiation into adipogenic, chondrogenic, neuronal or osteogenic lineages²⁶. Owing to the choice of PEG as an encapsulation material and the low concentration of functional groups relative to the PEG backbone, we were able to maintain a constant material compliance for this work and focus exclusively on changes in cell behaviour due to chemical functionality. Our results indicate that differentiation potential can be controlled through simple interactions with chemical functional groups rather than more complex soluble or tethered biomolecules, which would make production of therapeutic materials simpler, cheaper and more easily controlled. To our knowledge, this is the first example in which confounding factors such as materials properties and differences in cell morphology are eliminated and a synthetic matrix alone can be shown to control induction of multiple hMSC lineages purely through interactions with small-molecule chemical functional groups.

METHODS

Unless otherwise noted, all materials were obtained from Sigma-Aldrich and used without further purification.

PREPARATION OF SUBSTRATE AND ARRAYS OF CHEMICAL MOIETIES

Standard glass slides were cleaned using 'piranha' solution, dip-coated with 6 wt% poly(2-hydroxyethylmethacrylate) in methanol to render the glass surfaces non-cell-adhesive²⁹ and dried in a vacuum oven at 60 °C for at least 2 h.

Arrays of polymer spots were prepared from solutions containing PEG (molecular weight ~ 550) and 0.5, 5 or 50 mM of the monomethacrylated monomers 2-aminoethyl methacrylate, *t*-butyl methacrylate, ethylene glycol methacrylate phosphate, 2,2,3,3 tetrafluoropropyl methacrylate and methacrylic acid. The structures of these molecules are shown in Fig. 1a. I651 (Ciba-Geigy), an ultraviolet initiator, was added to these solutions at a concentration of 0.5 wt%. These solutions were spotted onto the poly(2-hydroxyethylmethacrylate)-coated slides using the Bio-Rad VersArray ChipWriter Pro System to create either 16 × 6 arrays with different concentrations (0.5, 5 and 50 mM) of each moiety for immunostaining screening or 6 × 6 arrays of the 50 mM concentrations for FISH analyses. The monomer spots were polymerized with ~4 mW cm⁻² ultraviolet light to create polymer gels for subsequent cellular analyses.

MESENCHYMAL STEM CELL CULTURE

hMSCs were purchased from Cambrex and cultured in low-glucose Dulbecco's modified eagle medium (Gibco) supplemented with 10% FBS (Invitrogen),

1% penicillin/streptomycin (Gibco), 0.25% gentamicin (Gibco) and 0.25% fungizone (Gibco). hMSCs at passage 3 were used in this study.

ASSESSING DIFFERENTIATION OF hMSCs ON CHEMICAL MOIETY ARRAYS

Immunostaining for proteins associated with differentiation of hMSCs was carried out. 16 × 6 arrays were sterilized by exposure to ultraviolet light, copiously washed with PBS to remove any unreacted monomers, and seeded with hMSCs at 20,000 cells cm⁻². After 10 days of culture, cells were rinsed in PBS and fixed in 4% paraformaldehyde. Antigen retrieval (PPARG only) was carried out by incubating sections in boiling citric acid (10 mM) for 10 min. The samples were blocked in 10% normal goat serum and 0.5% BSA for 30 min, incubated separately in primary antibodies (mouse anti-human collagen II (Abcam), osteopontin (Abcam) or PPARG (Abcam)) at 1:1,000 for 4 h, then incubated in secondary antibody (goat anti-mouse Alexa Fluor 532 (Molecular Probes)) at 1:100 for 2 h. Samples were mounted with ProLong Gold antifade reagent with propidium iodide (Molecular Probes) and allowed to cure overnight. Fluorescent images were taken with a Bio-Rad VersArray ChipReader and evaluated for the intensity of staining, normalized to the number of cells as indicated by propidium iodide staining, with a threshold for analyses of 2 × background.

Differentiation of hMSCs was analysed by FISH. Arrays were sterilized by exposure to ultraviolet light, copiously washed with PBS to remove any unreacted monomers and seeded with hMSCs at 20,000 cells cm⁻². After 4 and 10 days of culture, cells were rinsed in PBS and permeabilized in cytoskeletal buffer (100 mM NaCl, 300 mM sucrose, 3 mM MgCl₂, 10 mM PIPES, pH 6.8), cytoskeletal buffer plus 0.5% Triton X-100 and cytoskeletal buffer for 30 s each step. Cells were then fixed in 4% paraformaldehyde for 10 min and stored at -80 °C for up to 2 weeks. For FISH, samples were hybridized overnight in a humidity chamber at 65 °C. Probe production details and sequences are listed in the Supplementary Information.

Probes were prepared by hybridizing one target probe (Cy5-labelled) with β -actin (Cy3-labelled) with each array. After hybridization, slides were washed in 10% formamide, 2 × saline sodium citrate buffer (20 × SSC: 3 M NaCl, 0.3 M sodium citrate, pH 7), at 39 °C for 3 × 5 min and 2 × SSC for 3 × 5 min, and at room temperature using 1 × SSC for 10 min and 4 × SSC for 5 min with agitation. Fluorescent images were taken with a Bio-Rad VersArray ChipReader and evaluated for the intensity of staining, normalized to the intensity of β -actin, with a threshold for analyses of 2 × background.

hMSC attachment and spreading on different materials was monitored after 10 days in culture by staining the F-actin filaments with phalloidin. Samples were rinsed with PBS and fixed in 4% paraformaldehyde in PBS for 10 min. Fixed cells were permeabilized with 0.1% Triton X-100 in PBS for 5 min. Tetramethyl rhodamine isothiocyanate (TRITC) phalloidin (Chemicon) was diluted 1:100 each in PBS and samples were incubated for 1 h at room temperature, and mounted with ProLong Gold antifade reagent with 4,6-diamidino-2-phenylindole (DAPI; Molecular Probes) and allowed to cure overnight.

CHEMICAL-MOIETY EFFECTS ON ENCAPSULATED hMSC DIFFERENTIATION

hMSCs were photoencapsulated in a 10 wt% monomer solution in PBS; the solution contained PEG4600DM and 0.05 wt% photoinitiator I2959, a cyto-compatible photoencapsulation strategy³⁰. In addition, *t*-butyl methacrylate and ethylene glycol methacrylate phosphate were added separately at 50 mM to assess moiety effects on hMSC adipogenic and osteogenic differentiation in 3D culture. Cell/monomer solution (40 μ l) containing 25 × 10⁶ cells ml⁻¹ was polymerized in moulds on ultraviolet light exposure (~5 mW cm⁻², 10 min, 365 nm). After polymerization, the constructs were placed in hMSC media and cultured at 37 °C and 5% CO₂, replacing the media every 3–4 days. Directly after polymerization and after 4, 10 and 21 days, constructs were removed from culture and analysed for CBFA1 and PPARG protein production by immunoblotting using β -actin for normalization (anti-CBFA1 and anti-PPARG, Abcam; anti- β -actin, Sigma).

After 21 days of culture, cell-hydrogel constructs were fixed overnight in 4% paraformaldehyde in PBS, transferred to 22 wt% sucrose for 72 h, frozen in Cryo-gel (Instrumedics, Inc.) and cryosectioned (10 μ m sections). The sections were stained using Masson's trichrome, which stains collagen blue, and with Oil red, which stains intracellular lipid deposits red. All histological chemicals were obtained from Sigma. Immunohistochemistry was used to visualize osteopontin and PPARG. Antigen retrieval (PPARG only) was carried out by incubating sections in boiling citric acid buffer (10 mM) for 10 min and endogenous peroxidase activity was quenched by incubating in 3% H₂O₂

for 5 min. The slides were blocked in 10% normal goat serum and 0.5% BSA for 30 min, incubated separately in primary antibodies (mouse anti-human osteopontin (Abcam) or PPARG (Abcam)) at 1:100 for 4 h, then incubated in secondary antibody (goat anti-mouse horseradish peroxidase (Chemicon)) at 1:750 for 2 h. The sections were developed using Vector NovaRED Substrate Kit (Vector Labs). The sections were mounted with ProLong Gold antifade reagent (Molecular Probes) and allowed to cure overnight and imaged using conventional fluorescence microscopy (Nikon Eclipse TE300 and associated SPOT software).

Received 12 May 2007; accepted 28 July 2008; published 24 August 2008.

References

- Amis, E. J. Combinatorial materials science: Reaching beyond discovery. *Nature Mater.* **3**, 83–85 (2004).
- Bianco, P., Riminucci, M., Gronthos, S. & Robey, P. G. Bone marrow stromal stem cells: Nature, biology, and potential applications. *Stem Cells* **19**, 180–192 (2001).
- Meredith, J. C. et al. Combinatorial characterization of cell interactions with polymer surfaces. *J. Biomed. Mater. Res. A* **66**, 483–490 (2003).
- Saha, K., Pollock, J. F., Schaffer, D. V. & Healy, K. E. Designing synthetic materials to control stem cell phenotype. *Curr. Opin. Chem. Biol.* **11**, 381–387 (2007).
- Anderson, D. G., Levenberg, S. & Langer, R. Nanoliter-scale synthesis of arrayed biomaterials and its application to human embryonic stem cells. *Nature Biotechnol.* **22**, 863–866 (2004).
- Keselowsky, B. G., Collard, D. M. & Garcia, A. J. Surface chemistry modulates fibronectin conformation and directs integrin binding and specificity to control cell adhesion. *J. Biomed. Mater. Res. A* **66**, 247–259 (2003).
- Meyer, U. et al. Attachment kinetics and differentiation of osteoblasts on different biomaterials. *Cells Mater.* **3**, 129–140 (1993).
- Vanwachen, P. B. et al. Adhesion of cultured human-endothelial cells onto methacrylate polymers with varying surface wettability and charge. *Biomaterials* **8**, 323–328 (1987).
- Webb, K., Hlady, V. & Tresco, P. A. Relative importance of surface wettability and charged functional groups on NIH 3T3 fibroblast attachment, spreading, and cytoskeletal organization. *J. Biomed. Mater. Res. A* **41**, 422–430 (1998).
- Nuttelman, C. R., Benoit, D. S. W., Tripodi, M. C. & Anseth, K. S. The effect of ethylene glycol methacrylate phosphate in PEG hydrogels on mineralization and viability of encapsulated hMSCs. *Biomaterials* **27**, 1377–1386 (2006).
- Flaim, C. J., Chien, S. & Bhatia, S. N. An extracellular matrix microarray for probing cellular differentiation. *Nature Methods* **2**, 119–125 (2005).
- Anderson, D. G., Putnam, D., Lavik, E. B., Mahmood, T. A. & Langer, R. Biomaterial microarrays: rapid, microscale screening of polymer-cell interaction. *Biomaterials* **26**, 4892–4897 (2005).
- Engler, A. J., Sen, S., Sweeney, H. L. & Discher, D. E. Matrix elasticity directs stem cell lineage specification. *Cell* **126**, 677–689 (2006).
- McBeath, R., Pirone, D. M., Nelson, C. M., Bhadriraju, K. & Chen, C. S. Cell shape, cytoskeletal tension, and RhoA regulate stem cell lineage commitment. *Dev. Cell* **6**, 483–495 (2003).
- Caplan, A. L. Mesenchymal stem cells: Cell-based reconstructive therapy in orthopedics. *Tissue Eng.* **11**, 1198–1211 (2005).
- Barry, F. P. & Murphy, J. M. Mesenchymal stem cells: clinical applications and biological characterization. *Int. J. Biochem. Cell Biol.* **36**, 568–584 (2004).
- Kuo, C. K. & Tuan, R. S. Tissue engineering with mesenchymal stem cells. *IEEE Eng. Med. Biol. Mag.* **22**, 51–56 (2003).
- Herring, G. M. Chemical structure of tendon cartilage dentin and bone matrix. *Clin. Orthop. Rel. Res.* **60**, 261–299 (1968).
- Murphy, W. L. & Mooney, D. J. Bioinspired growth of crystalline carbonate apatite on biodegradable polymer substrate. *J. Am. Chem. Soc.* **124**, 1910–1917 (2002).
- Goldrick, R. B. Morphological changes in adipocyte during fat deposition and mobilization. *Am. J. Physiol.* **212**, 777–782 (1967).
- Rearson, M. F., Goldrick, R. B. & Fidge, N. H. Dependence of rates of lipolysis, esterification, and free fatty-acid release in isolated fat-cells on age, cell size, and nutritional state. *J. Lipid Res.* **14**, 319–326 (1973).
- Mackay, A. M. et al. Chondrogenic differentiation of cultured human mesenchymal stem cells from marrow. *Tissue Eng.* **4**, 415–428 (1998).
- Mayne, R., Vail, M. S., Mayne, P. M. & Miller, E. J. Changes in type of collagen synthesized as clones of chick chondrocytes grow and eventually lose division capacity. *Proc. Natl. Acad. Sci. USA* **73**, 1674–1678 (1976).
- Burdick, J. A. & Anseth, K. S. Photoencapsulation of osteoblasts in injectable RGD-modified PEG hydrogels for bone tissue engineering. *Biomaterials* **23**, 4315–4323 (2002).
- Bryant, S. J. & Anseth, K. S. Hydrogel properties influence ECM production by chondrocytes photoencapsulated in poly(ethylene glycol) hydrogels. *J. Biomed. Mater. Res.* **59**, 63–72 (2002).
- Beqaj, S., Jakkaraju, S., Mattingly, R. R., Pan, D. & Schuger, L. High RhoA activity maintains the undifferentiated mesenchymal cell phenotype, whereas RhoA down-regulation by laminin-2 induces smooth muscle myogenesis. *J. Cell Biol.* **156**, 893–903 (2002).
- Chastain, S. R., Kundu, A. K., Dhar, S., Calvert, J. W. & Putnam, A. J. Adhesion of mesenchymal stem cells to polymer scaffolds occurs via distinct ECM ligands and controls their osteogenic differentiation. *J. Biomed. Mater. Res. A* **78**, 73–85 (2006).
- Mandrup, S. & Lane, M. D. Regulating adipogenesis. *J. Biol. Chem.* **272**, 5367–5370 (1997).
- Selvarajan, S., Lund, L. R., Takeuchi, T., Craik, C. S. & Werb, Z. A plasma kallikrein-dependent plasminogen cascade required for adipocyte differentiation. *Nature Cell Biol.* **3**, 267–275 (2001).
- Smas, C. M. & Sul, H. S. Control of adipocyte differentiation. *Biochem. J.* **309**, 697–710 (1995).
- Gregoire, F. M., Smas, C. M. & Sul, H. S. Understanding adipocyte differentiation. *Physiol. Rev.* **78**, 783–809 (1998).
- Spiegelman, B. M. & Ginty, C. A. Fibronectin modulation of cell-shape and lipogenic gene-expression in 3T3-adipocytes. *Cell* **35**, 657–666 (1983).
- Mann, B. K., Gobin, A. S., Tsai, A. T., Schmedlen, R. H. & West, J. L. Smooth muscle cell growth in photopolymerized hydrogels with cell adhesive and proteolytically degradable domains: synthetic ECM analogs for tissue engineering. *Biomaterials* **22**, 3045–3051 (2001).
- Gobin, A. S. & West, J. L. Val-ala-pro-gly, an elastin-derived non-integrin ligand: Smooth muscle cell adhesion and specificity. *J. Biomed. Mater. Res. A* **67**, 255–259 (2003).
- DeLong, S. A., Gobin, A. S. & West, J. L. Covalent immobilization of RGDS on hydrogel surfaces to direct cell alignment and migration. *J. Control. Release* **109**, 139–148 (2005).

36. Gobin, A. S. & West, J. L. Effects of epidermal growth factor on fibroblast migration through biomimetic hydrogels. *Biotechnol. Prog.* **19**, 1781–1785 (2003).
37. Benoit, D. S. W. & Anseth, K. S. The effect on osteoblast function of colocalized RGD and PHSRN epitopes on PEG surfaces. *Biomaterials* **26**, 5209–5220 (2005).
38. Masters, K. S., Shah, D. N., Walker, G., Leinwand, L. A. & Anseth, K. S. Designing scaffolds for valvular interstitial cells: Cell adhesion and function on naturally derived materials. *J. Biomed. Mater. Res. A* **71**, 172–180 (2004).
39. Benoit, D. S. W., Nuttelman, C. R., Collins, S. D. & Anseth, K. S. Synthesis and characterization of a fluvastatin-releasing hydrogel delivery system to modulate hMSC differentiation and function for bone regeneration. *Biomaterials* **27**, 6102–6110 (2006).
40. Benoit, D. S. W. & Anseth, K. S. Heparin functionalized PEG gels that modulate protein adsorption for hMSC adhesion and differentiation. *Acta Biomater.* **1**, 461–470 (2005).
41. Bryant, S. J., Arthur, J. A. & Anseth, K. S. Incorporation of tissue-specific molecules alters chondrocyte metabolism and gene expression in photocrosslinked hydrogels. *Acta Biomater.* **1**, 243–252 (2005).

Supplementary Information accompanies the paper at www.nature.com/naturematerials.

Acknowledgements

This work was supported by a grant from the National Institute of Health (DE016523). The authors would like to thank C. Bowman and H. Sikes for use of and assistance with the ChipWriter, K. Rowlen and E. Dawson for use of and help with the ChipReader, E. Kovacs for technical assistance associated with *in situ* hybridization and J. McCormick and S. George for assistance with the X-ray photoelectron spectroscopy studies. Fellowship assistance to D.S.W.B. was awarded by the US Department of Education's Graduate Assistantships in Areas of National Need program and the National Science Foundation Graduate Research Fellowship program.

Author contributions

D.S.W.B. and K.S.A. came up with the concept, D.S.W.B., M.P.S. and K.S.A. designed the experiments, D.S.W.B. and A.R.D. carried out the experiments and D.S.W.B., M.P.S. and K.S.A. wrote the paper.

Author information

Reprints and permission information is available online at <http://npg.nature.com/reprintsandpermissions>. Correspondence and requests for materials should be addressed to K.S.A.